

COOLFluiD: an open computational platform for plasma and multi-physics

Andrea Lani



AMS seminar, 17th July 2014 @NASA Ames

Presentation Overview

COOLFluiD platform

- Project motivation & scope
- Design concepts & HPC
- High-resolution numerical algorithms

Aerothermodynamics modeling

- Atmospheric re-entry of space vehicles
- Experiments in high-enthalpy facilities

Astrophysical plasma modeling

- Ideal MHD for Space Weather
- Multi-fluid / Maxwell modeling

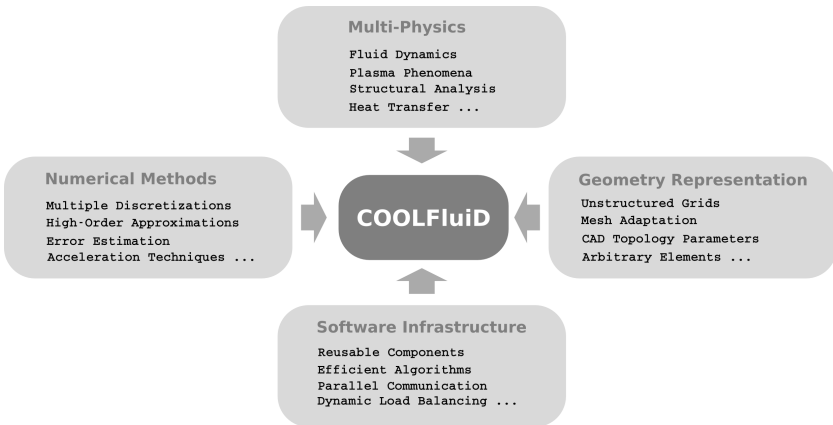
Gallery of other applications

- Other multi-physics applications

COOLFluiD platform

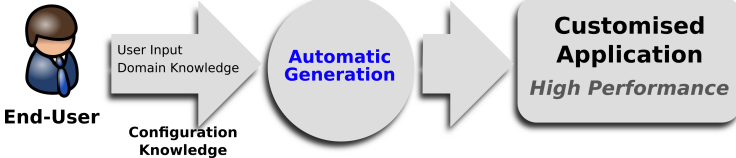
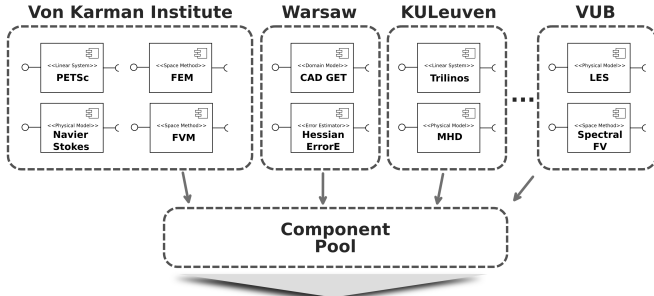
COOLFluiD platform (T. Quintino & A. Lani, 2002)

Combining and consolidate expertise from **multiple disciplines** ...



Collaborative Component-based Simulation Environment

... requires collaboration from **multiple partners!**



Capabilities

Multiple 1D/2D/3D parallel solvers for unstructured grids

- Time Steppers: RK-n, 1- & 3-point Backward Euler, CN, Limited
- **Multiple Space Discretizations:** FV, FE, RD, DG, Spectral FV/FD
- **Multiple Linear System Solvers:** PETSc, Trilinos, Pardiso, SAMG

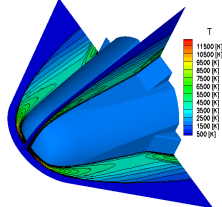
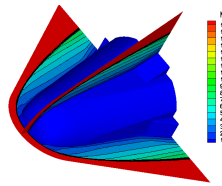
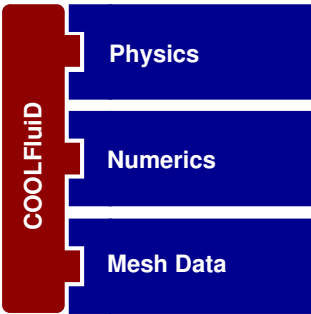
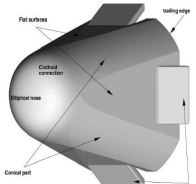
Multiple physical models

- Steady/unsteady **compressible and incompressible flows**
- Reactive flows: LTE, thermo-chemical nonequilibrium, ICP
- Magnetohydrodynamics (MHD), Maxwell, aeroacustics, RANS, LES
- Heat transfer, structural analysis, electro-chemistry

Multi-domain coupling amongst different models/algorithms

- Arbitrary Lagrangian Eulerian (ALE) with moving meshes
- Conjugate heat transfer, flow-radiation coupling (Monte Carlo)
- Aeroelasticity and aerothermoelasticity

Simplified conceptual view of COOLFluiD

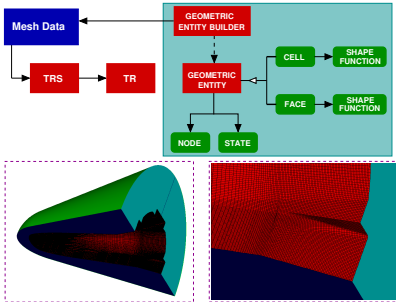
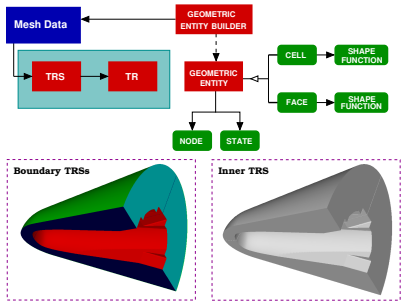


Input Mesh

CFD Simulation

Flowfield

MeshData \implies TRS & Geometric Entities

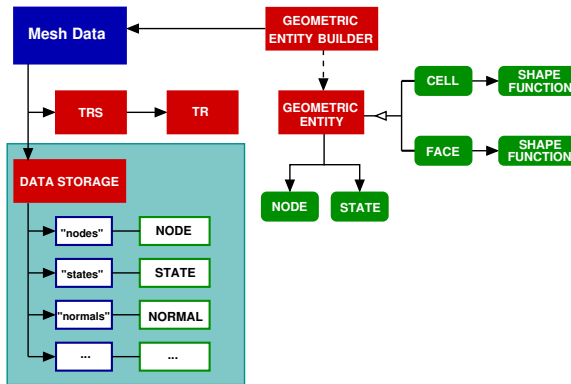


Topological Region Sets (TRS):
subdivisions of the computational domain

Geometric Entities: algorithm-dependent
agglomerations of DOFs

MeshData \implies Data Storage

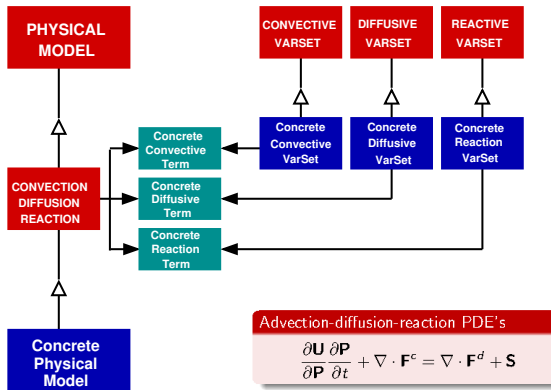
Facade managing **serial/parallel** data creation and access



Underlying data arrays can be **allocated on host and/or GPU device**

Physics \implies Perspective pattern for generic PDE's

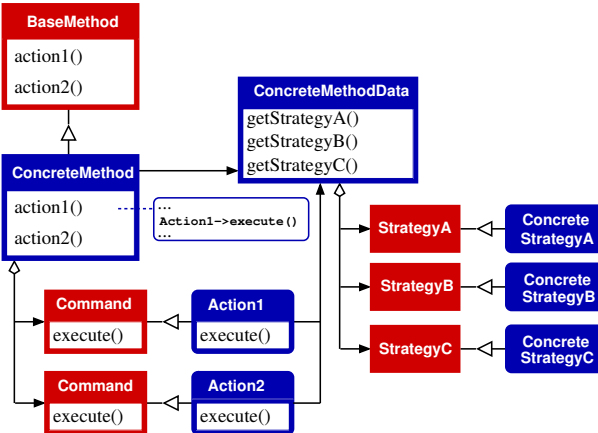
Multiple interfaces offering **multiple views** of the **same** physics



PDE's are decomposed into **Terms**, **Variable Sets** & **Transformers**

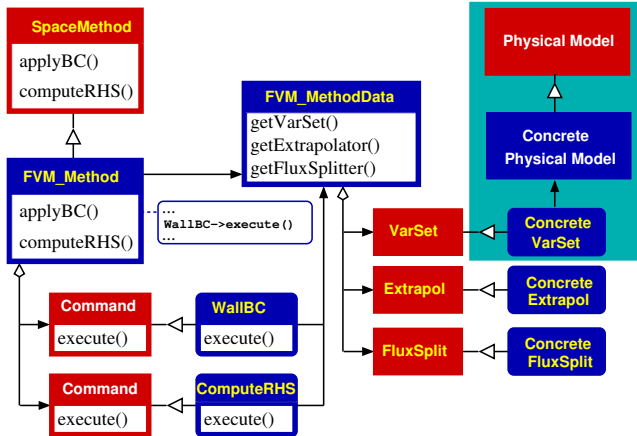
Numerics \implies Method Command Strategy (MCS) pattern

Flexible and **uniform** way to implement numerical algorithms



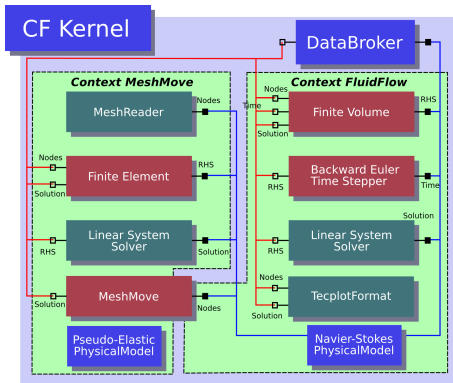
Physics + Numerics \implies MCS + Perspective Pattern

Flexible and uniform way to implement numerical algorithms



Components are connected via Data Sockets & Contexts

Numerical modules **provide/share generic data** via source/sink sockets

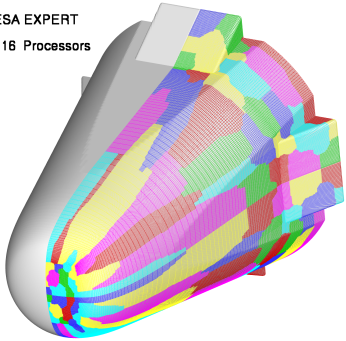


Contexts define the **collaboration domain** for data, physics and numerics

Parallel infrastructure for large scale HPC

ESA EXPERT

316 Processors



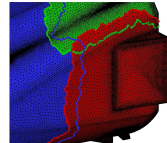
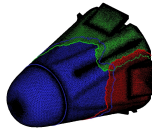
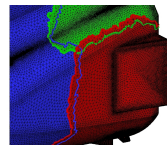
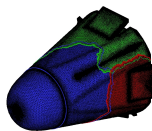
Parallel mesh partitioning with **ParMetis**

N-layer overlap region for customizable inter-process data exchange

Scalability tested up to 4,000 CPUs

Parallel I/O: reading and writing

Hybrid parallelization for CPU/GPU



Implicit Time Stepping

Newton Linearization

$$\tilde{\mathbf{R}}(\mathbf{P}) = \frac{\partial \mathbf{U}}{\partial \mathbf{P}} \frac{\partial \mathbf{P}}{\partial t} + \mathbf{R}(\mathbf{P}) = 0 \implies \left[\frac{\partial \tilde{\mathbf{R}}}{\partial \mathbf{P}} (\mathbf{P}^k) \right] \Delta \mathbf{P}^k = -\tilde{\mathbf{R}}(\mathbf{P}^k)$$

Implicit time integration schemes

$$\tilde{\mathbf{R}}(\mathbf{P}) = \frac{\mathbf{U}(\mathbf{P}) - \mathbf{U}(\mathbf{P}^n)}{\Delta t} \Omega + \mathbf{R}(\mathbf{P}) \quad \text{Backward Euler}$$

$$\tilde{\mathbf{R}}(\mathbf{P}) = \frac{\mathbf{U}(\mathbf{P}) - \mathbf{U}(\mathbf{P}^n)}{\Delta t} \Omega + \frac{1}{2} [\mathbf{R}(\mathbf{P}) + \mathbf{R}(\mathbf{P}^n)] \quad \text{Crank-Nicholson}$$

$$\tilde{\mathbf{R}}(\mathbf{P}) = \frac{3\mathbf{U}(\mathbf{P}) - 4\mathbf{U}(\mathbf{P}^n) + \mathbf{U}(\mathbf{P}^{n-1})}{2\Delta t} \Omega + \mathbf{R}(\mathbf{P}) \quad \text{3-Point Backward}$$

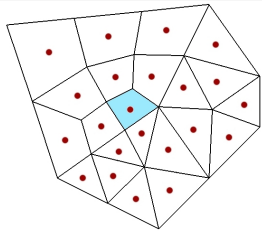
Linear system solvers (e.g. PETSc, Trilinos)

- GMRES solver
- Matrix storing and Matrix free
- Parallel preconditioners: ASM, ILU, B-Jacobi, etc.

Finite Volume Method (\mathcal{FV}), cell centered

$$\frac{d}{dt} \int_{\Omega_i} \mathbf{u} d\Omega_i + \oint_{\partial\Omega_i} \mathbf{F}^c \cdot \mathbf{n} d\partial\Omega_i = \oint_{\partial\Omega_i} \mathbf{F}^d \cdot \mathbf{n} d\partial\Omega_i + \int_{\Omega_i} \mathbf{s} d\Omega_i$$

$$\frac{\partial \mathbf{U}}{\partial \mathbf{P}}(\mathbf{P}_i) \frac{d\mathbf{P}_i}{dt} \Omega_i + \mathbf{R}^{FV}(\mathbf{P}_i) = 0$$



Cell-centered discretization

$$\mathbf{R}^{FV}(\mathbf{P}_i) = \sum_{f=1}^{N_f} \mathbf{F}_f^c \Sigma_f - \sum_{f=1}^{N_f} \mathbf{F}_f^d \Sigma_f - \mathbf{s}_i \Omega_i$$

Linear Reconstruction + Flux Limiter Φ

$$\tilde{\mathbf{P}}(\mathbf{x}_q) = \mathbf{P}_i + \Phi_i \nabla \mathbf{P}_i \cdot (\mathbf{x}_q - \mathbf{x}_i)$$

Upwind schemes for interface convective flux

$$\mathbf{F}_f^c = \begin{cases} \frac{1}{2} [\mathbf{F}_R^c + \mathbf{F}_L^c - |\bar{\mathbf{A}}| (\mathbf{u}_R - \mathbf{u}_L)] & \text{Roe} \\ \mathbf{F}^+ + \mathbf{F}^- = \mathbf{A}^+ \mathbf{u}_L + \mathbf{A}^- \mathbf{u}_R & \text{S-W} \\ \dot{m}_{1/2} \Psi_{L/R} + \mathbf{p}_{1/2} & \text{AUSM} \end{cases}$$

Central discretization for interface diffusive flux

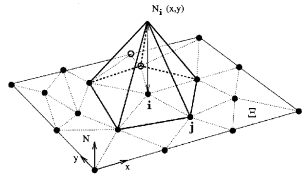
$$\begin{aligned} \mathbf{F}_f^d &= \mathbf{F}^d(\mathbf{P}_f, \nabla \mathbf{P}_f, \mathbf{n}_f) \\ \nabla \mathbf{P}_f &= \frac{1}{\Omega^V} \oint_{\Sigma^V} \mathbf{P} \mathbf{n} d\Sigma^V = \frac{1}{\Omega^V} \sum_{s=1}^{N_I} \bar{\mathbf{P}}_s \mathbf{n}_I \Sigma_I^V \end{aligned}$$

Residual Distribution Method (\mathcal{RD}), vertex centered

$$\frac{\partial \mathbf{U}}{\partial \mathbf{P}}(\mathbf{P}_I) \frac{d\mathbf{P}_I}{dt} V_I + \mathbf{R}^{RD}(\mathbf{P}_I) = 0$$

FEM linear interpolation

$$\mathbf{P}^h(\mathbf{x}, t) = \sum_{j=1}^d \mathbf{P}_j(t) N_j(\mathbf{x}), \quad N_j(\mathbf{x}_k) = \delta_{jk}$$



Galerkin discretization of diffusive term

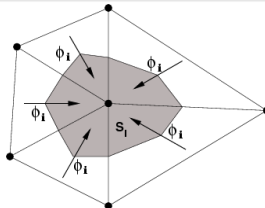
$$\Phi_I^d = - \sum_{\Omega \in \Xi_I} \frac{1}{\Omega d} \int_{\Omega} \mathbf{F}^d(\mathbf{P}, \nabla \tilde{\mathbf{P}}) \cdot \mathbf{n}_I \, d\Omega$$

Vertex-centered discretization

$$\mathbf{R}^{RD}(\mathbf{P}_I) = \Phi_I^c - \Phi_I^d - \Phi_I^s$$

Discretization of convective term

$$\Phi_I^c = \sum_{\Omega \in \Xi_I} \mathbf{B}_I^\Omega(\mathbf{K}^\pm) \Phi^{c,\Omega}$$

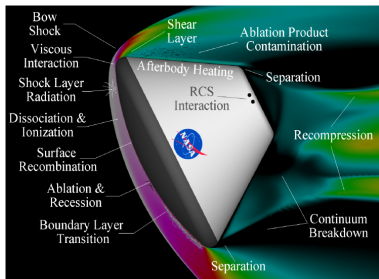


Petrov-Galerkin discretization of source term

$$\Phi_I^s = \sum_{\Omega \in \Xi_I} \int_{\Omega} \mathbf{w}_I^\Omega \cdot \mathbf{s} \, d\Omega \stackrel{1\text{-point}}{\Rightarrow} \sum_{\Omega \in \Xi_I} \mathbf{B}_I^\Omega \mathbf{s}_c \cdot \mathbf{\Omega}$$

Aerothermodynamics modeling

What is Aerothermodynamics?



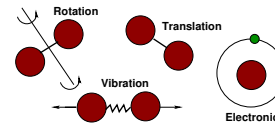
Flowfield surrounding a re-entry capsule (courtesy of D. Hash).

Truly multi-physical science

- gasdynamics
- statistical thermodynamics
- chemical kinetics
- quantum mechanics

Thermo-chemical regimes ($Da = \tau_f / \tau_c$)

- ① Frozen flows $(Da \approx 0)$
- ② Equilibrium flows $(Da \gg 1)$
- ③ Nonequilibrium flows $(Da \approx 1)$



Different systems of PDE's

- Non-reacting Navier-Stokes
- LTE-FEF or LTE-VEF
- TCNEQ (multi-temperature)

Chemical Equilibrium (LTE) & Nonequilibrium (CNEQ)

Flow is modeled as a **mixture** of N_s perfect gases

$$p = \sum_{s \neq e} p_s + p_e, \quad p_s = \rho_s \frac{R}{M_s} T, \quad p_e = \frac{R}{M_e} T_e, \quad \rho_s = \rho y_s$$

Example of gas mixtures

- **Nitrogen-2:** N, N_2
- **Air-11:** $e^-, N, O, N_2, NO, O_2, N^+, O^+, N_2^+, NO^+, O_2^+$
- **Mars-18 (CR):** $e^-, C^*, N^*, O^*, N_2, O_2, NO, CO, CO_2, C_2, CN, C^+, N^+, O^+, N_2^+, O_2^+, CO^+, NO^+$

Chemical models

- **Equilibrium (LTE):** $y_s = y_s(p, T, Y_e)$
 - ▶ LTE-FEF: $Y_e = \text{const}$
 - ▶ LTE-VEF: $\frac{\partial \rho Y_e}{\partial t} + \nabla \cdot (\rho Y_e \mathbf{u}) = -\nabla \cdot (\rho \mathbf{J}_e)$
- **Nonequilibrium:** $\frac{\partial \rho y_s}{\partial t} + \nabla \cdot (\rho_s \mathbf{u}) = -\nabla \cdot (\rho_s \mathbf{u}_s^d) + \dot{\omega}_s$

Thermal Nonequilibrium (TCNEQ)

Energy disequilibration amongst different modes (**separation** assumption)

$$e = e_t(T_t) + e_e(T_e) + e_f \quad \text{atoms}$$

$$e = e_t(T_t) + e_r(T_r) + e_v(T_{v,m}) + e_e(T_e) \quad \text{molecules}$$

$$e = e_t(T_e) \quad \text{free electrons}$$

Examples of multi-temperature models

- 3-T model (ionized mixtures): $T_t = T_r = T$, $T_{v,m} = T_v$, T_e
- 2-T model (ionized mixtures): $T_t = T_r = T$, $T_{v,m} = T_e = T_{ve}$
- Multi-T (neutral mixtures): $T_t = T_r = T$, $T_{v,m}$

Prototype electron-electronic or vibrational energy conservation equation

$$\frac{\partial \rho e_*}{\partial t} + \nabla \cdot (\rho e_* \mathbf{u}) = \Omega_*$$

Governing equations for TCNEQ

Advection-diffusion-reaction PDE's

$$\frac{\partial \mathbf{U}}{\partial \mathbf{P}} \frac{\partial \mathbf{P}}{\partial t} + \nabla \cdot \mathbf{F}^c = \nabla \cdot \mathbf{F}^d + \mathbf{S}$$

Conservative and natural variables for Multi-T model

$$\mathbf{U} = [\rho_s \ \rho \mathbf{u} \ \rho E \ \rho_m e_{v,m} \ \rho e_e]^T \quad \mathbf{P} = [\rho_s \ \mathbf{u} \ T \ T_{v,m} \ T_e]^T$$

Fluxes and Source Terms for Multi-T model (ionized mixture)

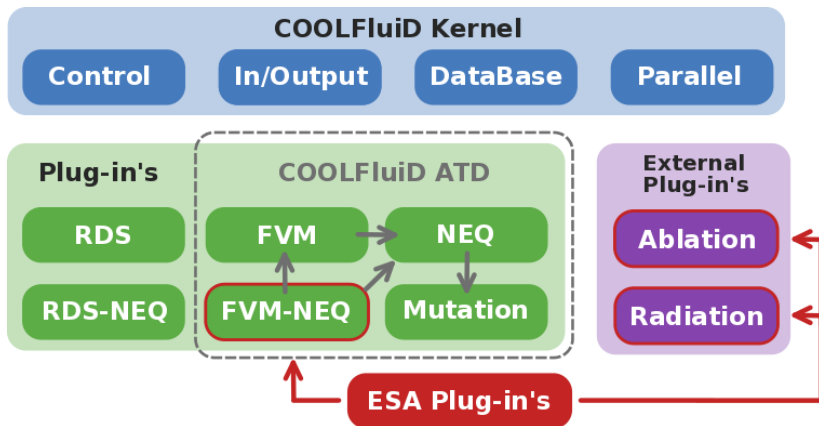
$$\mathbf{F}^c = \begin{pmatrix} \rho_s \mathbf{u} \\ \rho \mathbf{u} H \\ \rho_m \mathbf{u} e_{v,m} \\ \rho e_e \end{pmatrix}, \quad \mathbf{F}^d = \begin{pmatrix} -\frac{\rho_s \mathbf{u}_s}{\tilde{\tau}} \\ (\tilde{\tau}^{-1} \cdot \mathbf{u})^T - \sum_s \rho_s \mathbf{u}_s h_s - \mathbf{q} \\ -\rho_m \mathbf{u}_m h_{v,m} - \mathbf{q}_{v,m} \\ -\sum_s \rho_s \mathbf{u}_s h_{e,s} - \mathbf{q}_e \end{pmatrix}, \quad \mathbf{S} = \begin{pmatrix} \omega_s \\ 0 \\ -Q_{rad} \\ \Omega_m^{v,t} + \Omega_m^{v,e} + \Omega_m^{cv} + \Omega_m^{v,v} \\ -\rho_e \nabla \mathbf{u} + \Omega_e^t + \Omega_e^I - \sum_m \Omega_m^{v,e} - Q_{rad} \end{pmatrix}$$

MUTATION library by T. Magin (VKI) & M. Panesi (UIUC)

Computation of transport, thermodynamics, chemistry, energy transfer

COOLFluiD Aerothermodynamics

Customizable kernel designed for reusability & third party extensions

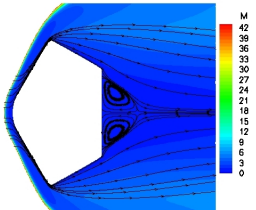


Stardust Sample Return Capsule

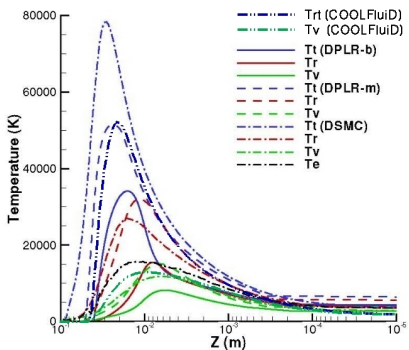
► Air-11, 2T (T , T_{ve}), $M_\infty = 42$ (Fastest re-entry!)



Stardust capsule after landing



Mach number, FV AUSM+

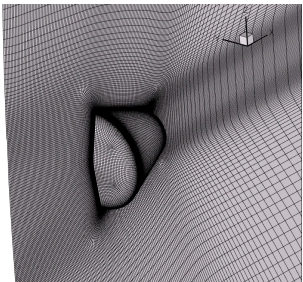


Stagnation temperatures profiles
COOLFluiD vs. NASA DPLR

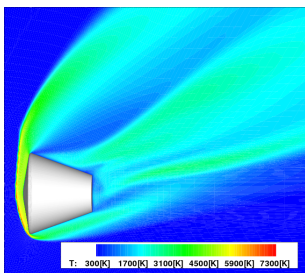
G. Degrez, A. Lani, M. Panesi et al., J. Phys. D: App. Phys., 2009.

ESA BLAST space capsule

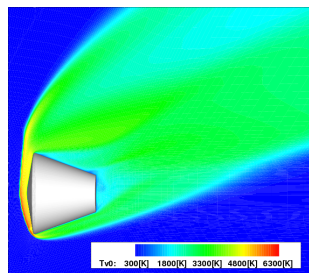
► Air-5, 2T (T , T_v), $M_\infty = 15$, $\alpha = 25^\circ$



Computational mesh
(4,363,072 hexa)



Roto-translational T
FV AUSM+



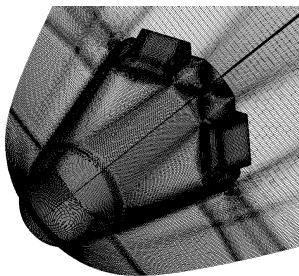
Vibrational T
FV AUSM+

ESA EXPERT (EXPERimental Re-entry Test-bed) vehicle

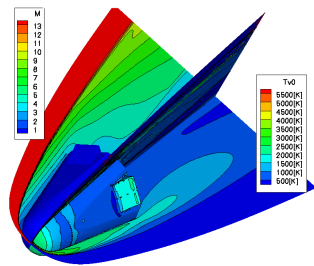
► Air-5, 2T (T , T_v), $M_\infty = 13.5$, $\alpha = 0^\circ$



EXPERT re-entry vehicle: to be launched soon



Computational mesh
(3,840,453 hexa)

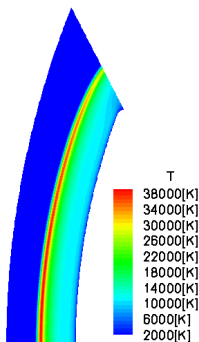


Mach number and T_v
FV AUSM+

M. Panesi, A. Lani et al., AIAA-2007-4317, 2007.

FIRE II experiment: Collisional Radiative (CR) models

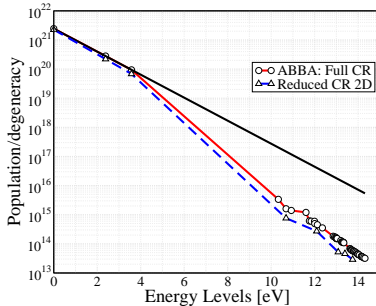
► Air-11, 2T (T , T_{ve}), $V_\infty = 11360$ [m/s], $\alpha_{esc} = 0$, $t=1634$ [s]



FIRE II launch

Roto-translational T
FV AUSM+

ABBA CR-116 (1D) vs CR-18 (2D)

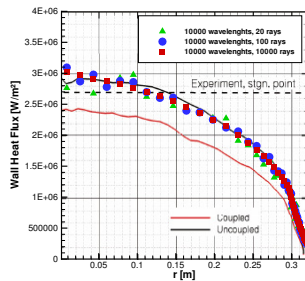
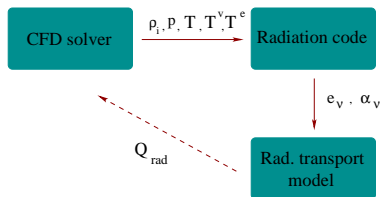


Electronic energy populations for N
at 1.0 cm from the shock front



FIRE II experiment: flow-radiation coupling

► Air-11, 2T (T , T_v), $U_\infty = 10480$ [km/s], $T_\infty = 276$ [K], $t=1643$ [s]



Flow-radiation coupling infrastructure

Radiative heat flux (FV + Monte Carlo)

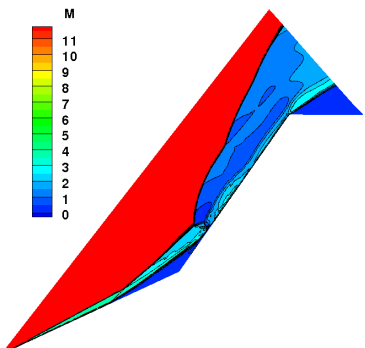
A. Lani, A. Sanna, N. Villedieu, M. Panesi, **WRHTG Barcelona**, 2012.

A. Lani, P. Duarte Santos, A. Sanna, **AIAA-2013-2893**, 2013.

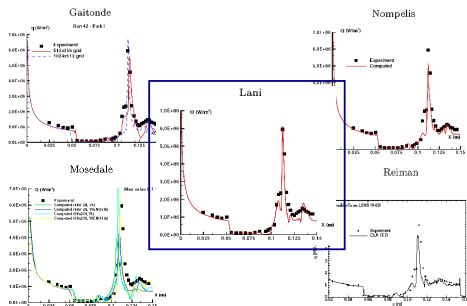
Experiments in high-enthalpy facilities

NATO STO experiments: double cone flows (AVT 136)

► Nitrogen-2, 2T ($T, T_{N_2}^v$), $M_\infty = 11.5$



Mach number field

Surface heat flux measurements:
COOLFluiD (CRD-Bx) vs. FV solvers

A. Lani and H. Deconinck, **AIAA-2009-460**, 2009.

A. Lani, M. Panesi and H. Deconinck, **J. Comm. Comput. Phys.**, 2013.

D. Knight, J. Longo, D. Drikakis, D. Gaitonde, A. Lani et al., **J. Progr. Aerospace Sciences**, 2012.



NATO STO experiments: double wedge flows (AVT 205)

► Air, perfect gas, $M_\infty = 7.11$, unsteady

Movie

Movie: temperature field

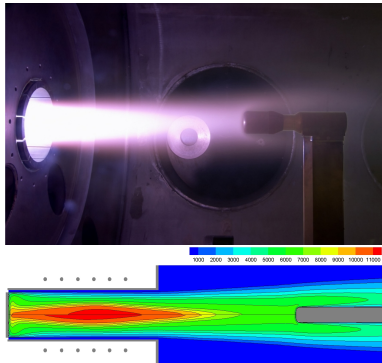
Movie

Movie: surface heat flux
FV vs. experiments ($t=0.327\ ms$)

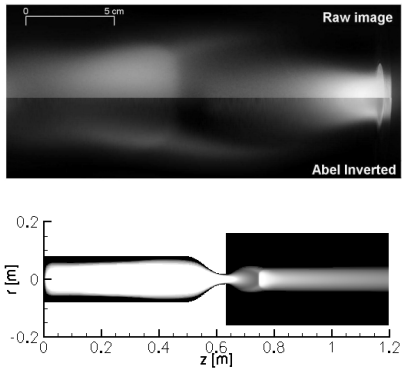
Inductively Coupled Plasma: testing in VKI Plasmatron

► Air-11, LTE, $\dot{m} = 8$ [g/s], $p = 10000$ [Pa], $P = 90$ [kW]

Incompressible subsonic testing



Incompressible to supersonic testing



Temperature field (**Sartori**)

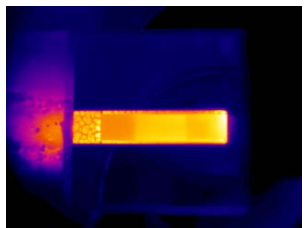
ICP-LTE solver, Rhee-Chow scheme

Temperature field (**V. Van der Haegen**)

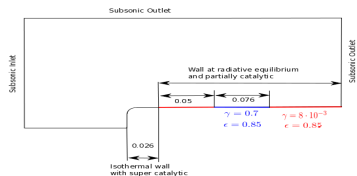
ICP-LTE solver, modified AUSM+up scheme

Gas-surface interaction: TPS testing in VKI Plasmatron

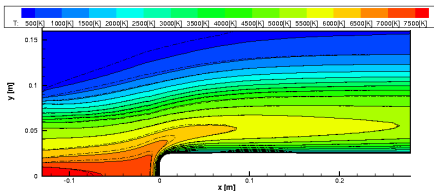
► Air-11, 2T (T , T_{ve}), variable catalycity efficiency γ



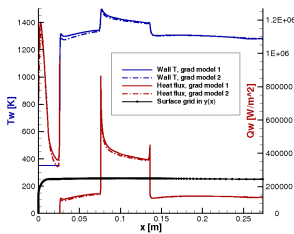
IR visualization (F. Panerai)



Numerical setup and BC's



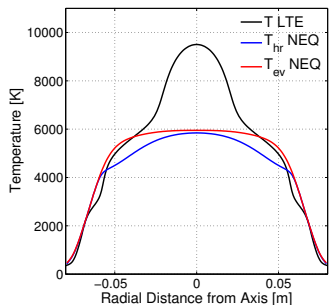
Temperature field, FV AUSM+



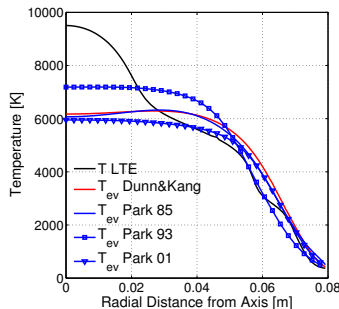
Surface temperature and heat flux

Inductively Coupled Plasma: TCNEQ effects in the torch

- NEQ effects inside the torch itself is not essential for TPS-testing purposes, provided LTE conditions are reached at the outlet
- Different equilibrium conditions are found by TCNEQ and LTE at low p
- Park 1993 predicts largest extent of TCNEQ (Dunn-Kang gives LTE)

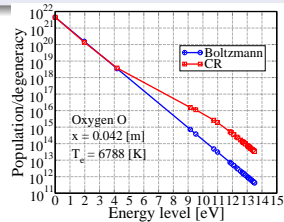
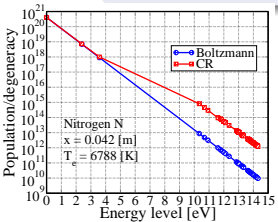
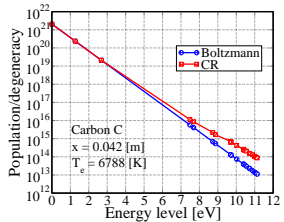
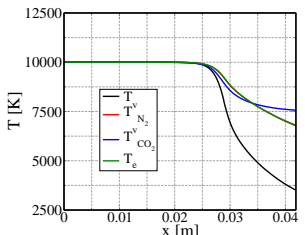


(a) Temperatures

(b) Effects of kinetic model on T_v

Expanding plasma experiments: VKI Minitorch

► Mars-18, 4T , $T_0 = 10^4 \text{ K}$, $p_0 = 1 \text{ atm}$, $\alpha_{esc} = 0$



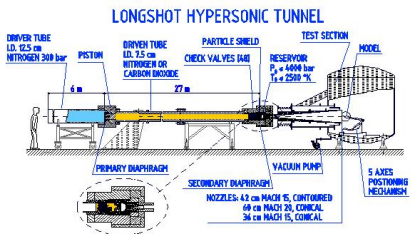
- Electronically-specific CR (**123 eqs!**)
- 1D FV AUSM+ MUSCL

In the figures:

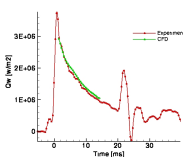
- Temperature profiles (left)
- Energy level populations (below)

Expanding hypersonic flows: VKI Longshot facility

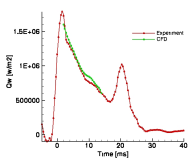
► Nitrogen, $P_0 = 3256.22 \text{ [Pa]}$, $T_0 = 2652.1 \text{ [K]}$



Movie: ALE simulation of the driven tube
(courtesy of K. Bensassi)



High Reynolds number.



Low Reynolds number.

Movie

Movie: expansion in nozzle up to M=14
Pressure, 3-point Backward Euler, FV Roe
(courtesy of K. Bensassi)

Stagnation heat flux: experiments vs. CFD

Astrophysical plasma modeling

Ideal MHD: $B_0 + B_1$ splitting technique

$$\vec{B}_{\text{(total magnetic field)}} = \vec{B}_0(r)_{\text{(planetary dipole magnetic field)}} + \vec{B}_1_{\text{(variable magnetic field)}}$$

MHD system of equations + Hyperbolic Divergence Cleaning (HDC)

$$\frac{\partial \mathbf{U}}{\partial \mathbf{P}} \frac{\partial \mathbf{P}}{\partial t} + \nabla \cdot \mathbf{F}_{MFS} + \nabla \cdot \mathbf{F}_{B_0 B_1} = 0$$

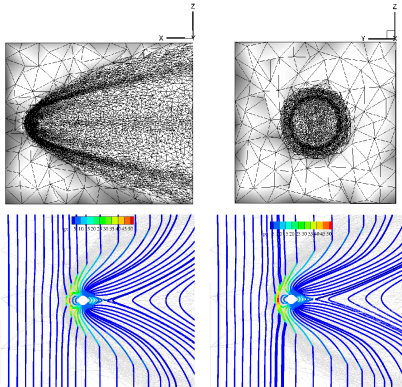
$$\mathbf{U} = \begin{pmatrix} \rho \\ \rho \vec{v} \\ \vec{B} \\ E_1 = E - \vec{B}_1 \cdot \vec{B}_0 - B_0^2/2 \\ \Phi \end{pmatrix}, \quad \mathbf{P} = \begin{pmatrix} \rho \\ \vec{v} \\ \vec{B} \\ p \\ \Phi \end{pmatrix}$$

$$\mathbf{F}_{B_0 B_1} = \begin{pmatrix} 0 \\ (\vec{B}_0 \cdot \vec{B}_1) \bar{\mathbf{I}} - (\vec{B}_0 \vec{B}_1 + \vec{B}_1 \vec{B}_0) \\ \vec{v} \vec{B}_0 - \vec{B}_0 \vec{v} \\ (\vec{B}_0 \cdot \vec{B}_1) \vec{v} - (\vec{v} \cdot \vec{B}_1) \vec{B}_0 \\ 0 \end{pmatrix}, \quad \mathbf{F}_{MFS} = \begin{pmatrix} \rho \vec{v} \\ \rho \vec{v} \vec{v} + (p + B_1^2/2) \bar{\mathbf{I}} - \vec{B}_1 \vec{B}_1 \\ \vec{v} \vec{B}_1 - \vec{B}_1 \vec{v} + \bar{\mathbf{I}} \Phi \\ (E_1 + p + B_1^2/2) \vec{v} - (\vec{v} \cdot \vec{B}_1) \vec{B}_1 \\ V_{ref}^2 \vec{B}_1 \end{pmatrix}$$

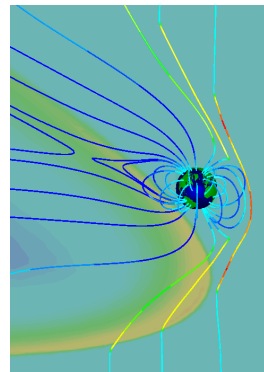
Solar wind/Earth magnetosphere interaction (steady)

$$\mathbf{V}_\infty = 780 \text{ km/s}, \mathbf{c}_\infty = 126 \text{ km/s}, \mathbf{n}_\infty = 5 \text{ cm}^{-3}, \mathbf{B}_{z\infty} = -10 \text{ nT}, \gamma = 5/3$$

Second-level adapted grid (2,013,946 tetrahedra)



Pressure variations over B field lines in xz-plane:
HDC (left) vs. Powell's source term approaches



Density variations over B field lines
and contours on the z=−20 plane.

M. S. Yalim et al, J. Comput. Phys., 2011.

Solar wind/Earth's magnetosphere interaction (unsteady)

06/04/00 magnetic storm, input based on the ACE satellite data

Movies: proton density and B lines (courtesy of **M. S. Yalim**).

Movie

Movie

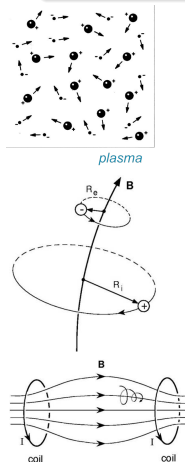
3-point Backward Euler, FV LF-HDC (**up to 2.5X faster on GPU**)

Integrated into the ESA **Virtual Space Weather Modeling Center**

A. Lani, M. S. Yalim and S. Poedts, **Comp. Phys. Comm.**, 2014.

Magnetized plasma modeling (A. Alvarez Laguna)

Plasma is a mixture of **charged particles** (ions and electrons) and **neutrals** that is affected by **external magnetic fields**



Magnetized plasma models

KINETIC THEORY	MULTI-FLUID THEORY	ONE-FLUID THEORY
<ul style="list-style-type: none"> ✓ Molecular scale resolution ✗ Computationally too costly for full scale representation 	<ul style="list-style-type: none"> ✓ Collisional and chemical effects ✓ Full-Scale phenomena representation 	<ul style="list-style-type: none"> ✗ No microphysics effects ✓ Full-Scale phenomena representation



Multi-fluid plasma

Each **species** α (ions, electrons, neutrals) has **its speed & temperature**

Fluid dynamics

$$\frac{\partial \mathbf{U}}{\partial \mathbf{P}} \frac{\partial \mathbf{P}}{\partial t} + \nabla \cdot \mathbf{F}^c = \nabla \cdot \mathbf{F}^d + \mathbf{S}$$

$$\mathbf{U} = [\rho_\alpha \quad \rho_\alpha \mathbf{u}_\alpha \quad \rho_\alpha E_\alpha]^T, \quad \mathbf{P} = [\rho_\alpha \quad \mathbf{u}_\alpha \quad T_\alpha]^T$$

$$\mathbf{F}^c = \begin{pmatrix} \rho_\alpha \mathbf{u}_\alpha \\ \rho_\alpha \mathbf{u}_\alpha \mathbf{u}_\alpha + p_\alpha \hat{\mathbf{I}} \\ \rho_\alpha \mathbf{u}_\alpha H_\alpha \end{pmatrix}, \quad \mathbf{F}^d = \begin{pmatrix} 0 \\ \bar{\tau}_\alpha \\ (\bar{\tau}_\alpha \cdot \mathbf{u}_\alpha)^T - \mathbf{q}_\alpha \end{pmatrix}$$

$$\mathbf{S} = \begin{pmatrix} \dot{m}_\alpha \\ Q_\alpha \vec{E} + \vec{j}_\alpha \times \vec{B} + \sum_{\beta \neq \alpha} \vec{R}_\alpha^{\alpha\beta} \\ \vec{j}_\alpha \cdot \vec{E} + \sum_{\beta \neq \alpha} \vec{R}_\alpha^{\alpha\beta} \cdot \mathbf{u}_\alpha + \sum_{\beta \neq \alpha} H_\alpha^{\alpha\beta} + \dot{Q}_\alpha \end{pmatrix}$$

Chemical reactions terms

Collisional terms

Maxwell-Fluid coupling terms

Maxwell + HDC

$$\frac{\partial \vec{B}}{\partial t} + \nabla \times \vec{E} + \gamma \nabla \psi = 0$$

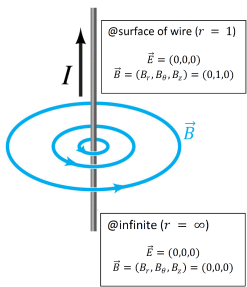
$$\frac{\partial \vec{E}}{\partial t} - c^2 \nabla \times \vec{B} + \chi c^2 \nabla \phi = - \frac{\vec{j}}{\epsilon_0}$$

$$\frac{\partial \psi}{\partial t} + \gamma c^2 \nabla \cdot \vec{B} = 0$$

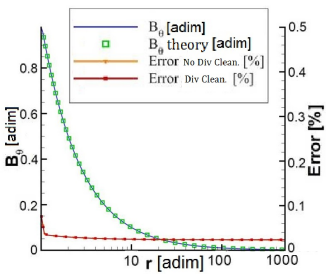
$$\frac{\partial \phi}{\partial t} + \chi \nabla \cdot \vec{E} = \chi \frac{\rho_c}{\epsilon_0}$$

- Two scalar fields ϕ and ψ
- Artificial waves at χc and γc clean divergence errors

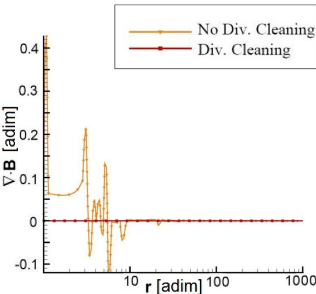
Maxwell: Induced B field around a wire carrying current



Azimuthal Magnetic Field
 B_θ versus radius

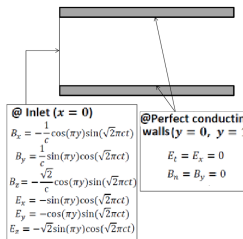


Divergence of magnetic field $\nabla \cdot \vec{B}$ versus radius

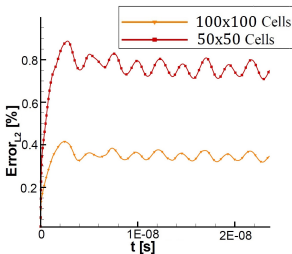


- Error $\left| \frac{B_{\theta_{theory}} - B_{\theta_{num}}}{B_{\theta_{theory}}} \right| < 0.1\%$ in a 18000 cells mesh
- Non-dimensional $|\nabla \cdot \vec{B}| \sim 10^{-13}$ using the HDC method

Maxwell: Electromagnetic 2D wave



Movie

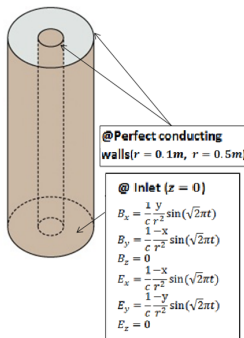


Evolution of the Electric Field E_x in time

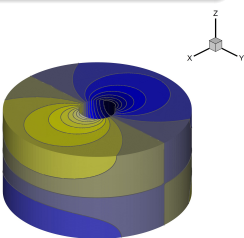
Global error evolution in time

- Case use to validate all the components of the electromagnetic field
- Error < 1% in a 50x50 mesh and < 0.5% in a 100x100 mesh

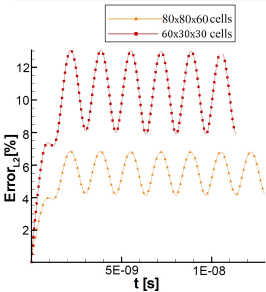
Maxwell: 3D coaxial waveguide



Snapshot of E_x solution



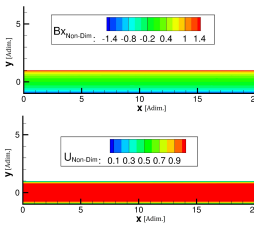
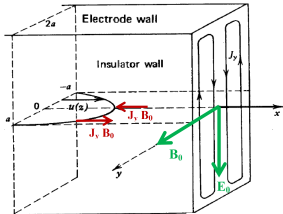
Global error evolution in time



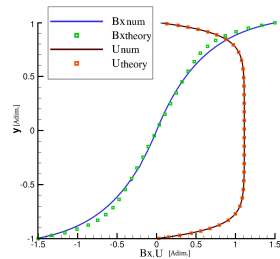
- Validation of **3D unsteady** solver
- Error $\sim 5\%$ in a $80\times 80\times 60$ mesh

Single-fluid: Hartmann flow

- Single conducting fluid affected by external E and B fields
- Magnetic field B_x is induced by the electric current.
- Velocity profile is not parabolic: local Lorentz forces flatten the profile.
- AUSM+up for the fluid, Munz's scheme for Maxwell.



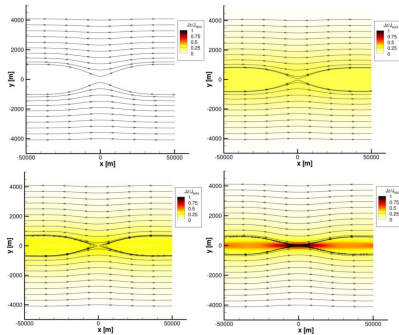
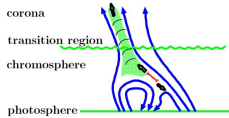
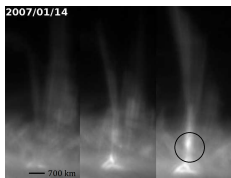
B_x and velocity steady solution



B_x and velocity profiles

Two-fluid: onset of chromospheric magnetic reconnection

- **Magnetic reconnection:** process by which the magnetic energy is transformed into thermal and kinetic energy
- **Two reacting fluid model:** considering charged particles + neutrals.

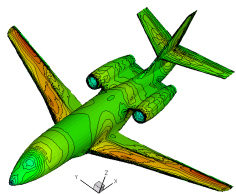


Gallery of other applications

Compressible external aerodynamics

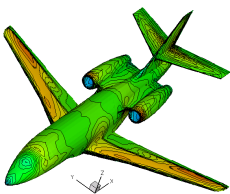
Multiple solvers for aeronautics applications

LDA/N scheme (RDS)



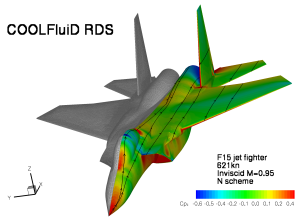
Falcon aircraft

2nd order Roe, Barth Limiter (FVM)



Falcon aircraft

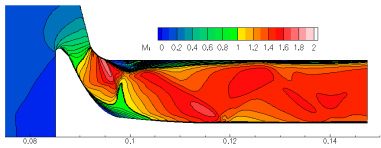
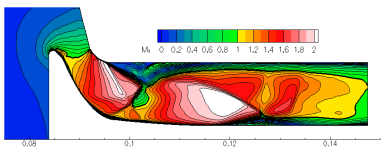
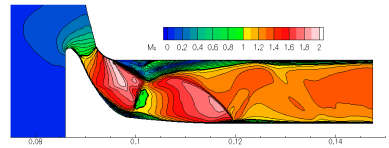
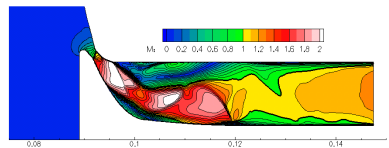
COOLFluiD RDS



F15 aircraft

Internal aerodynamics with moving geometries

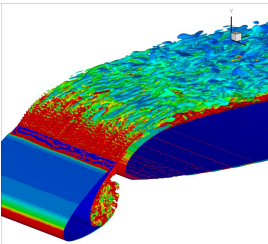
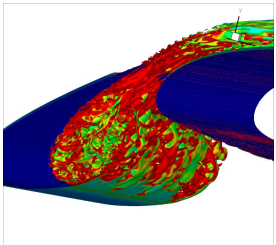
Arbitrary Lagrangian-Eulerian (ALE) formulation



Flow around an exhaust valve with URANS (courtesy of M. Zaloudek)

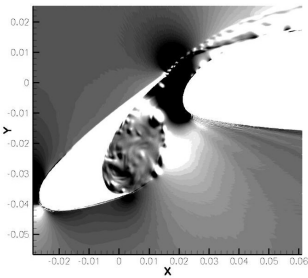
Turbulence modeling

Large Eddy Simulation (LES) with RD methods



Q iso-structures under
the wing colored by
vorticity magnitude

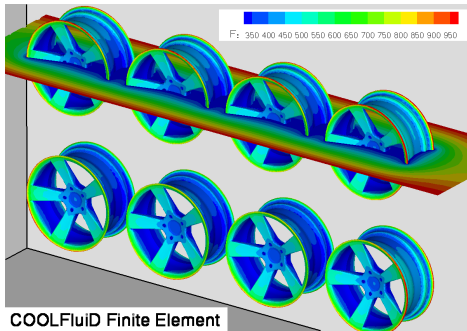
Q iso-structures on the
wing colored by
vorticity magnitude



Numerical Schlieren,
mid-plane view
(courtesy of L. Kapa)

FEM for electrochemistry

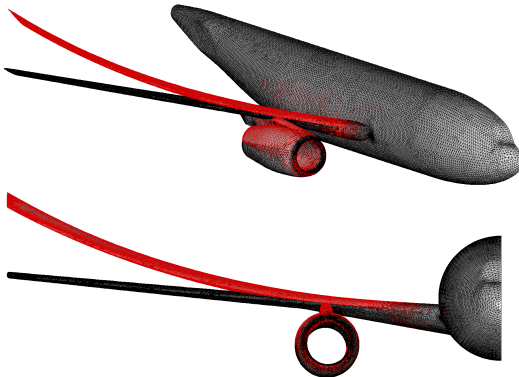
Electrochemical processes on complex geometries



Chromium deposition on car wheels (courtesy of **T. Quintino**)

FEM for structural analysis and fluid-structure interaction

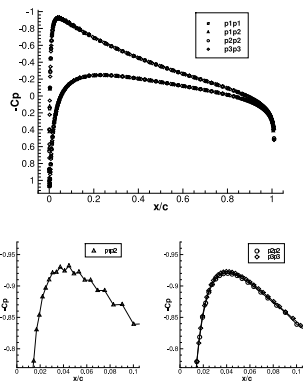
Linear and non-linear elasticity with high-order FEM



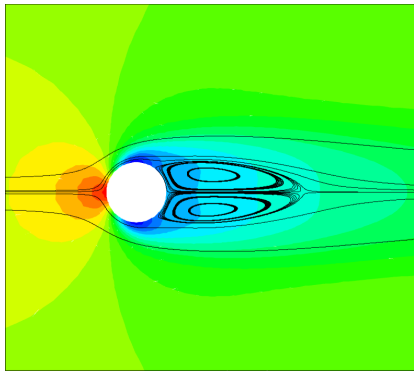
DLR F6 aircraft (courtesy of **T. Wuilbaut**)

High-Order numerical methods for aeronautics

Compressible inviscid and laminar flows



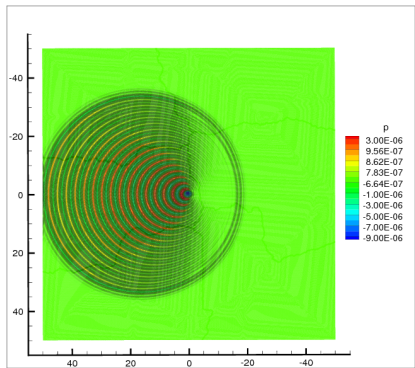
$2^{nd}, 3^{rd}, 4^{th}$ order RDS
 C_p on NACA0012 (**M. Vymazal**)



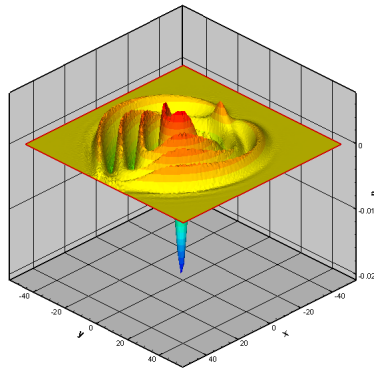
Spectral F. Differences 4th order
(courtesy of **K. Vanden Abeele**)

High-Order numerical methods for aeroacoustics

Linearized Euler for sound propagation

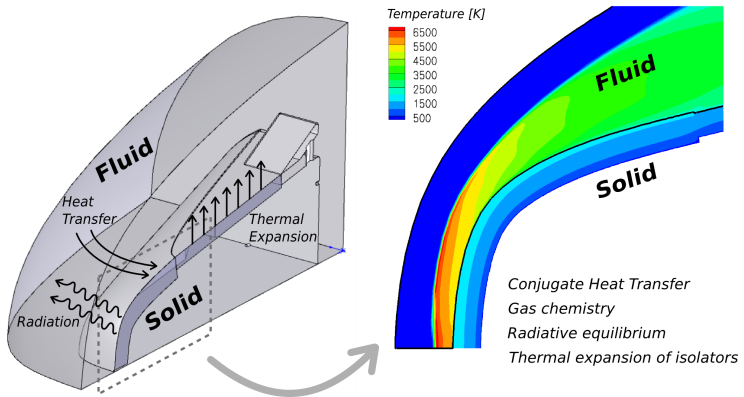


Monopole on uniform flow Ma 0.5
(courtesy of **L. Kapa**)



Monopole in a jet flow
(courtesy of **L. Kapa**)

ESA EXPERT: Aerothermoelastic study



- Chemical NEQ flow with FV
- Heat conduction in the solid with FEM
- Thermal expansion of the metallic cone with FEM
- Pseudo-elastic mesh deformation with FEM
- Non-matching interfaces

T. Wuilbaut, Ph.D. thesis, 2008.

Some statistics

COOLFluiD team and quick facts

- **15** defended & **5** ongoing PhD thesis
- **60+** **contributors** since 2002 from various institutions
- 1,000,000+ lines of codes, 100+ modules
- C++ / MPI / CUDA, interfaces to a few Fortran libraries
- **60+** **scientific publications** (journal & conference articles)
- 15+ funded projects so far (ESA, EU FP7, US AFOSR, national)
- Subversion repository, mailing list and website
- Partially **open source** under LGPL v3 license

Conclusions

Ongoing developments and collaborators

- Multi-fluid plasma models (N. Mansour, A. Kosovicev, S. Poedts)
- Plasma discharge facilities modeling (M. Panesi, N. Mansour)
- Shock fitting techniques for RD schemes (R. Paciorri, A. Bonfiglioli)
- Coupling of MHD and Particle-in-Cell solvers (S. Olshevsky)

Future developments & wish list

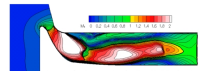
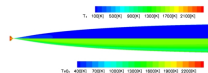
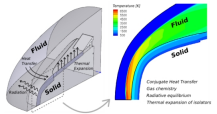
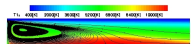
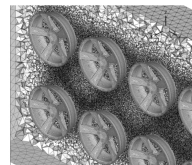
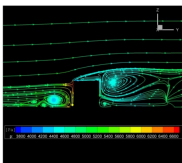
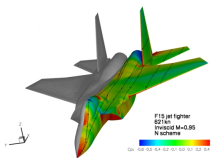
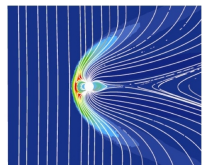
- Enhance hybrid parallelization and multi-domain infrastructure
- Re-meshing and dynamic mesh adaptation tools
- Higher order plasma solvers
- Flow-material-radiation coupling

Acknowledgments

- Former core developers: T. Quintino, D. Kimpe, T. Wuilbaut
- All contributors (students, engineers), Prof. Deconinck
- **FWO G.0729.11N grant** for the development of multi-fluid models.



Thank you all for the attention!



<http://coolfluidsrv.vki.ac.be/trac/coolfluid>